# Photonic-wireless Communication and Sensing in the Terahertz Band

**Xianbin Yu[1,*], Hongqi Zhang[1], Zuomin Yang[1], Zhidong Lyu[1], Hang Yang[1], Yuqian He[1], Siqi Liu[1], Nan Li[1], Oskars Ozolins[2], Xiaodan Pang[2], Lu Zhang[1], Xianmin Zhang[1]**
[1]*College of Information Science and Electronic Engineering, Zhejiang University, Hangzhou 310027, China.*
[2]*Royal Institute of Technology, SE-10044, Stockholm, Sweden*
*Author e-mail address: xyu@zju.edu.cn*

**Abstract:** This paper reviews the potential of THz photonics in communication and sensing by presenting our experimental results in the 300-500 GHz. Benefiting from the large available bandwidth in both THz and photonics, THz communications with high speed and THz imaging with high resolution have been achieved. 

## 1. Introduction

With the rapid development of terahertz (THz) devices in electronics and photonics in recent years, THz frequency band has attracted increasing attention. The main research directions contain THz high-speed wireless communication [1], THz radar [2], as well as THz imaging [3], and so on. However, the electronically-generated THz signals usually lack frequency tunability and are restrained by the available bandwidth. Alternatively, photonics-assisted techniques exhibit the capability of breaking the electronic bandwidth bottleneck. Significant progress has been made in the field of THz communication, radar, and imaging. With regards to THz communication, THz wave is recognized as a strong candidate to realize ultra-fast wireless communication. For instance, wireless transmissions of 100 Gbit/s at 280 GHz [4], 106 Gbit/s at 400 GHz [5], and 128 Gbit/s at 300 GHz [6] over 0.5 m have been demonstrated. It is also noted that THz radar has the following advantages compared with microwave radar. First, radar signals with a larger bandwidth can be loaded onto THz carriers, enabling high-resolution imaging. In addition, the short wavelength and narrow antenna beam of the THz wave can, in principle, achieve higher antenna gain and better angular resolution, hence improving the ability of target recognition [7]. With the help of THz photonic technology, we have proposed a method to generate a linear frequency modulated (LFM) signal with large bandwidth in [8,9] to improve the radar resolution. Furthermore, THz imaging, as a part of sensing applications, also attracts increasing attention recently, as it can provide both amplitude and phase information of the samples [10,11].

In this paper, we overview the potential of THz waves in enabling high-speed wireless communication and high-resolution sensing by presenting two photonics-assisted THz wireless links, a THz photonic inverse synthetic aperture radar (ISAR) system, and a continuous-wave THz vector imaging system in the 300-500 GHz band. The net rates of communication systems respectively reach 100.8 Gbit/s and 510.5 Gbit/s, and the imaging resolution of radar system reaches 7 mm × 7 mm.

## 2. THz communication

Fig. 1(a) depicts the 100.8 Gbit/s photonics-based THz communication link. Here two optical carriers with an interval of 350 GHz are fed into the UTC-PD for generating THz signals. The modulation format of the baseband signal is 16-ary quadrature amplitude modulation (16-QAM) combined with orthogonal frequency-division multiplexing (OFDM) and probabilistic shaping (PS) technique, named PS-16-QAM-OFDM. A Schottky diode mixer is used to down-convert the received THz signals into the intermediate frequency (IF) domain. Fig. 1(b), (c) shows the experimental results. The BER performance can reach the SD-FEC threshold, and a net transmission capacity of 100.8 Gbit/s is successfully obtained after wireless transmission over 26.8 m.

The experimental configuration of the 600 Gbit/s THz wireless system is depicted in Fig. 2 (a) [13]. One optical carrier from an external cavity laser (ECL-1) is used to generate an optical frequency comb (OFC) for subsequent WDM strategy. Here the modulation format of PS-64-QAM-OFDM is employed to improve the spectral efficiency. After the signal modulation, the optically modulated signals are coupled with another optical carrier from the ECL-2, and the combined signals are then sent to the UTC-PD-X and Y to generate X-Pol, and Y-Pol THz signals, respectively. Fig. 2(b) shows the measured BER performance under different incident optical power, and the BER performance of two polarization directions (X-Pol, Y-Pol) of two channels can both reach the SD-FEC threshold. A total line data rate is up to 612.65 Gbit/s in this case. The aggregated net data rate reaches 510.5 Gbit/s by taking the error-correction overhead into account. Fig. 2(c) shows the constellations of the PS-64-QAM format of each channel for both paths, and the spectral efficiency for the first channel of the X polarization path is 5.5 bit/symbol.

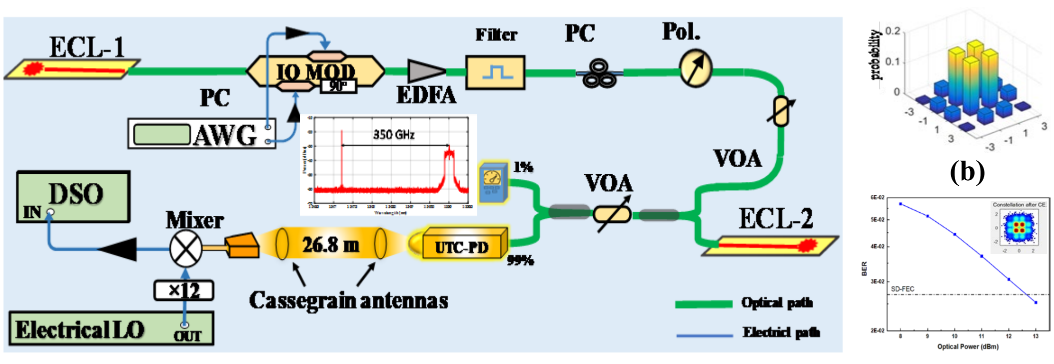


(a) (c)

Fig. 1 (a) Experimental configuration of photonics-based THz communication link [12]. The right: photos of actual THz wireless link. The insert: optical spectrum at the input of UTC-PD. (b) PS-16-QAM signals with an average information amount of 3.5 bit/symbol. (c) The measured transmission performance with the recovered PS-16-QAM constellation.

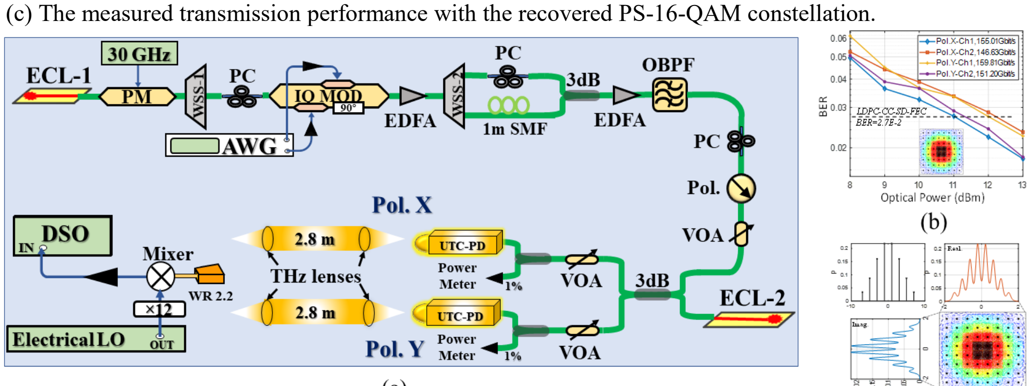


Fig. 2. (a) Experimental setup of 600 Gbit/s THz communication system [13]. (b) BER performance versus the optical power for two channels for X-Pol and Y-Pol. (c) Constellations of each channel for both two paths.

### 3. THz sensing

The experimental configuration of the THz photonic ISAR system is shown in Fig. 3(a) [14]. At the transmitter, the THz LFM signal at 324 GHz is generated from the UTC-PD. Then the THz signals are radiated toward an object. At the receiver side, a 12-order harmonics Schottky diode THz mixer is employed to down-convert the received THz echo signals into the IF domain. Finally, a real-time digital sampling oscilloscope (DSO) is used to sample the de-chirped signal based on optical modulation techniques. In this experiment, several aluminum pillars are placed on a rotating turntable, as shown in Fig. 3 (b) and (d). The turntable is 1.3 m away from the transmitter and receiver and rotates at the speed of 30 s per lap. After performing the 2-dimensional fast Fourier transform (FFT) on the data, the measured ISAR image is shown in Fig. 3(c) and (f). Both the number and the placement information of targets can be obtained from the imaging results, which are consistent with the actual arrangements.

Fig. 4 (a) shows the experimental setup for a continuous-wave THz vector imaging system [15]. The optical frequency comb (OFC) with an interval of 30 GHz and 6 GHz is generated by cascading a phase modulator (PM) and an intensity modulator (IM). After the selection of the waveshaper (WSS), three optical carriers are sent to the UTC-PD, and two THz carriers centered at 294 GHz, and 300 GHz are radiated. Then the THz wave passes through a sample and illuminates the THz receiver based on an SBD. Finally, the amplitude and phase of the THz signal are extracted using a lock-in amplifier (LIA). Fig. 4(b) and (c) depict the clear results of amplitude and phase imaging on ‘ZJU’ letters.

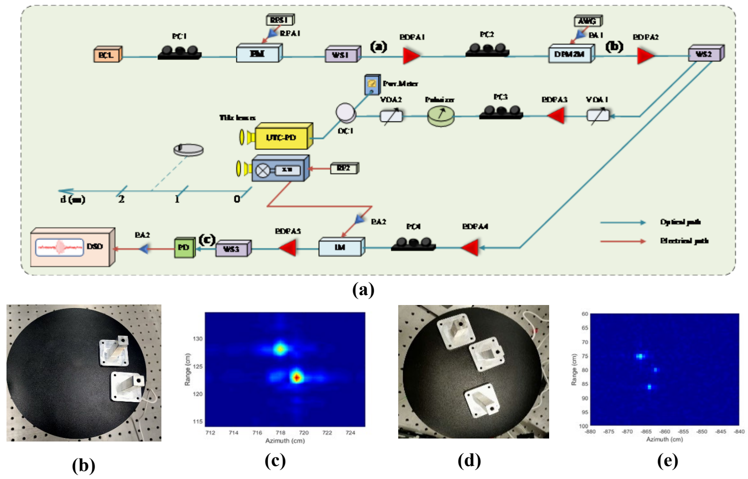


Fig. 3. (a) The experimental configuration of the THz photonic ISAR system [14]. (b) Photograph of aluminum pillars. (c) THz ISAR image of (b). (d) Photograph of aluminum pillars. (e) THz ISAR image of (d).

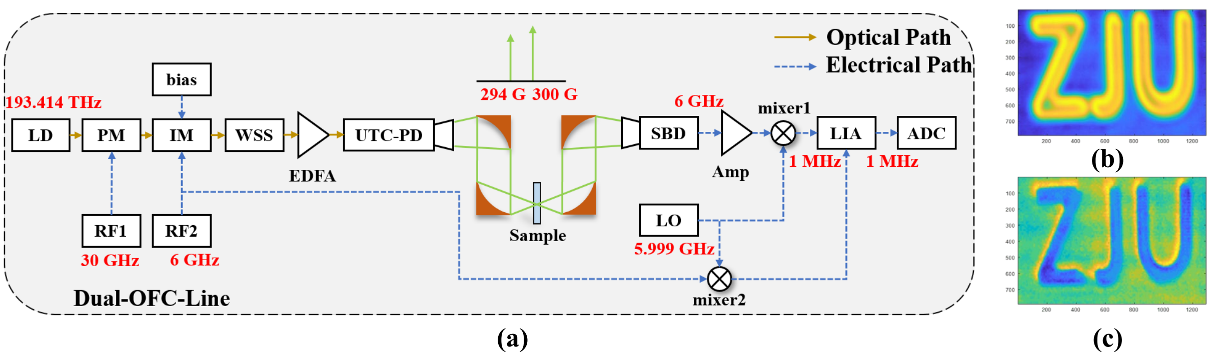


Fig. 4. (a) Experimental setup of THz vector imaging system. The imaging of (b) amplitude and (c) phase [15].

## 4. Conclusions

In summary, we have experimentally demonstrated some work on THz wireless communications and THz imaging in 300-500 GHz, both of which are supported by THz photonics. Benefiting from the large bandwidth of photonic technology, THz communications with high speed and THz imaging with high resolution can be achieved. More interestingly, it is foreseen that the convergence of both sensing and communication will serve as a promising direction for our smart future.


## Acknowledgments

This work is supported by the National Key Research and Development Program of China (2020YFB1805700), in part by the Natural National Science Foundation of China under Grants 62101483, the Natural Science Foundation of Zhejiang Province under Grant LQ21F010015, Zhejiang Lab (no. 2020LC0AD01), and the Swedish Research Council (VR) projects 2019-05197.


## References


[1] T. Nagatsuma, et al., in OFC, 2017, 1-90.
[2] C. Jansen, et al. Appl. Optics, **49**, E48-E57 (2010).
[3] V, Krozer, et al. IEEE T. Microw. Theory, **58**, 2027-2039 (2010).
[4] V. K. Chinni, et al., Electron. Lett. **54**, 638-640, (2018).
[5] S. Jia, et al., J. Light. Technol. **36**, 610-616, (2018).
[6] C. Castro, et al., in OFC, 2019, paper M4F. 5.
[7] F. Zhang, et al., Opt. Express **25**, 16274 (2017).
[8] H. Zhang, et al., Opt. Lett. **42**, 5242 (2017).
[9] S. Wang, et al., IEEE Photon. Technol. Lett. **31**, 881 (2019).
[10] H. Song, Optics Express **25**, 20718-20726 (2017).
[11] X. Gao, et al., In Proc SNOTA, 11455 (2020).
[12] S. Wang, et al., APL photonics, **5**, 056105 (2020).
[13] S. Jia, et al., J. Lightwave Technol. **38**, 4715-4721 (2020).
[14] S. Wang, et al., In Proc. OECC, 2021, pp. M3E-4.
[15] Z. Yang, et al., J. Lightwave Technol. **40**, 2717-2723 (2022).